

M87* IN SPACE, TIME AND FREQUENCY

DYNAMIC VLBI IMAGING WITH INFORMATION FIELD THEORY

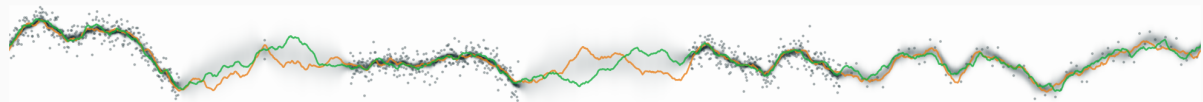
Philipp Arras, Philipp Frank, Jakob Knollmüller

June 28, 2021

Ludwig-Maximilians Universität LMU, Munich, Germany

Technical University TUM, Munich, Germany

Max-Planck Institute for Astrophysics, Garching, Germany



ACKNOWLEDGEMENTS

Our focus:

- Philipp Arras (TUM/MPA): radio imaging algorithms
- Jakob Knollmüller (TUM): approximate inference, machine learning
- Philipp Frank (LMU/MPA): statistical methods

Our co-authors:

- Philipp Haim (LMU/MPA): medical imaging
- Reimar Leike (LMU/MPA): galactic dust, machine learning
- Martin Reinecke (MPA): numerical algorithms
- Torsten Enßlin (MPA): head of *information field theory* group

LMU: Ludwig-Maximilians Universität München

TUM: Technical University Munich

MPA: Max-Planck Institute for Astrophysics, Garching

ORGANISATIONAL

- The talk is structured into three main parts:
 1. Overview and results (Philipp Arras)
 2. Prior and likelihood (Philipp Frank)
 3. Inference scheme and validation (Jakob Knollmüller)
- The presentation material (including the videos) is available at:
<https://philipp-arras.de/2021cfa.html>
- Our paper [AFH⁺20] is available at:
<https://arxiv.org/abs/2002.05218>
- The imaging code is available under GPL license (see link in paper).

STARTING SITUATION

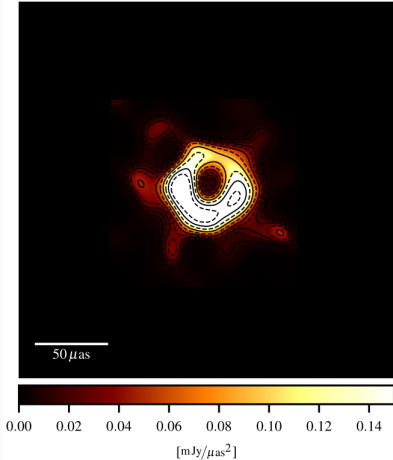
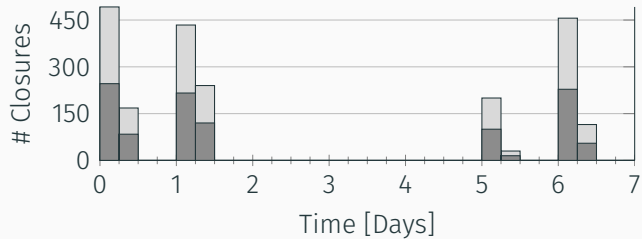


Figure 1: M87* on day 0 imaged with ehtimaging [AAA⁺19b]. Saturated color bar.

- Uncertainty quantification via multiple independent imaging teams
- Independent imaging for each observing day



Product Rule of Probabilities

aka Bayes' theorem

$$\mathcal{P}(s|d) = \frac{\mathcal{P}(d|s) \mathcal{P}(s)}{\mathcal{P}(d)}$$

$\mathcal{P}(A|B)$: conditional probability,
s: parameters, d: data.

(Some) assumptions

- The brightness is strictly positive.
- The source features correlation in spatial, temporal and frequency direction.

⇒ Encoded in $\mathcal{P}(s)$.

Product Rule of Probabilities

aka Bayes' theorem

$$\mathcal{P}(s|d) = \frac{\mathcal{P}(d|s) \mathcal{P}(s)}{\mathcal{P}(d)}$$

$\mathcal{P}(A|B)$: conditional probability,
s: parameters, d: data.

In our case

- Correlation structure → full 4d-movie: sky brightness has shape (2, 28, 256, 256).
- The posterior $\mathcal{P}(s|d)$ is a ridiculously high-dimensional function:

$$\begin{cases} \mathbb{R}^{7,500,000} & \rightarrow \mathbb{R}^{\geq 0} \\ s & \mapsto \mathcal{P}(s|d) \end{cases}$$

- This function encodes our knowledge on M87* including uncertainties.

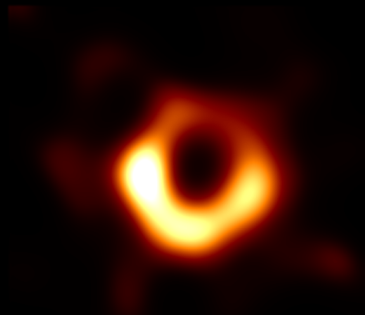
(Some) assumptions

- The brightness is strictly positive.
- The source features correlation in spatial, temporal and frequency direction.
⇒ Encoded in $\mathcal{P}(s)$.





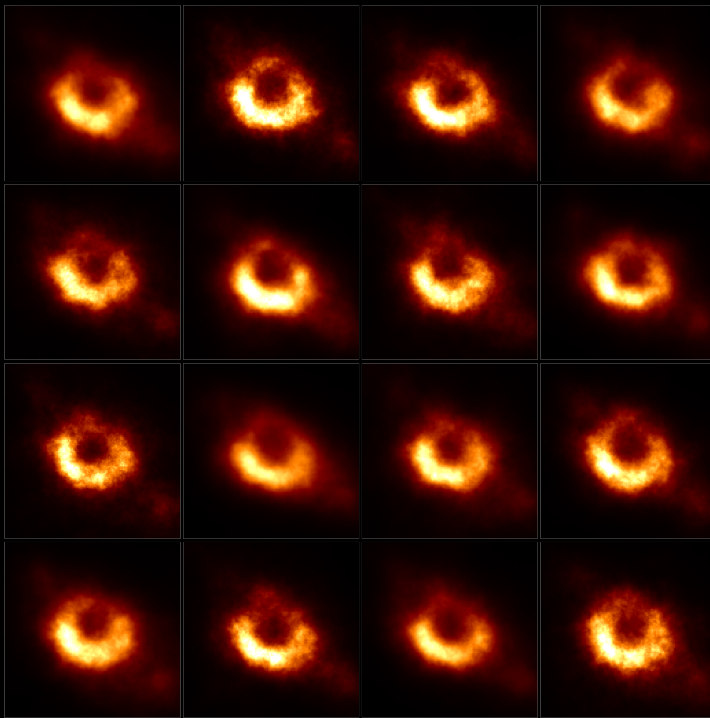








vlbi-resolve, [AFH⁺20], posterior mean.



vlbi-resolve, [AFH⁺20], 16 posterior samples.

DATA CONSISTENCY

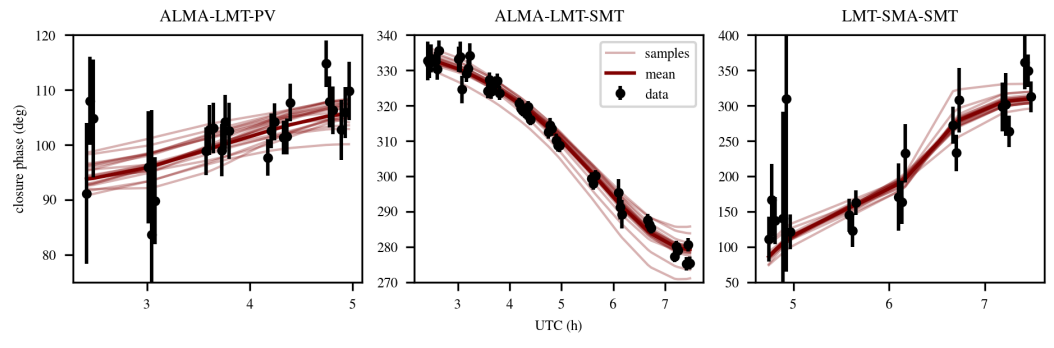


Figure 2: Three closure phases for triples of antennas as a function of time.

RING FITTING (SEE [AAA⁺19B, TABLE 7])

	d (μ as)	w (μ as)	η ($^{\circ}$)	A	f_c
EHT-IMAGING [AAA ⁺ 19b]					
April 5	39.3 ± 1.6	16.2 ± 2.0	148.3 ± 4.8	0.25 ± 0.02	0.08
April 6	39.6 ± 1.8	16.2 ± 1.7	151.1 ± 8.6	0.25 ± 0.02	0.06
April 10	40.7 ± 1.6	15.7 ± 2.0	171.2 ± 6.9	0.23 ± 0.03	0.04
April 11	41.0 ± 1.4	15.5 ± 1.8	168.0 ± 6.9	0.20 ± 0.02	0.04
OUR METHOD					
UNCERTAINTY AS PER [AAA ⁺ 19B, TABLE 7])					
April 5	44.4 ± 3.4	23.2 ± 5.2	164.9 ± 9.5	0.26 ± 0.04	0.365
April 6	44.4 ± 2.9	23.3 ± 5.4	161.7 ± 5.6	0.24 ± 0.04	0.374
April 10	44.8 ± 2.8	23.0 ± 5.0	176.7 ± 9.8	0.22 ± 0.03	0.374
April 11	44.6 ± 2.8	22.8 ± 4.8	180.1 ± 10.4	0.22 ± 0.03	0.372
SAMPLE UNCERTAINTY					
April 5	44.1 ± 1.2	23.1 ± 2.4	163.9 ± 5.0	0.25 ± 0.03	0.377 ± 0.081
April 6	44.0 ± 1.2	22.9 ± 2.4	161.9 ± 6.0	0.24 ± 0.03	0.385 ± 0.085
April 10	44.6 ± 1.2	22.9 ± 2.5	176.2 ± 6.5	0.22 ± 0.03	0.383 ± 0.089
April 11	44.6 ± 1.2	23.0 ± 2.6	179.8 ± 6.2	0.22 ± 0.03	0.383 ± 0.090

RESULTS

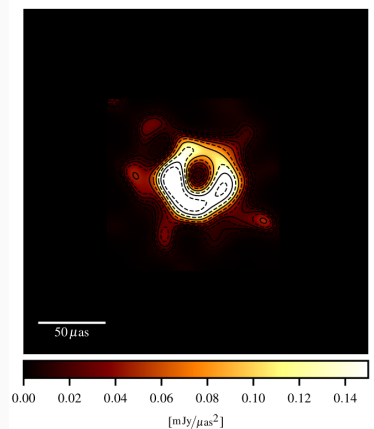


Figure 3: M87* on day 0 imaged with ehtimaging [AAA⁺19b]. Saturated color bar.

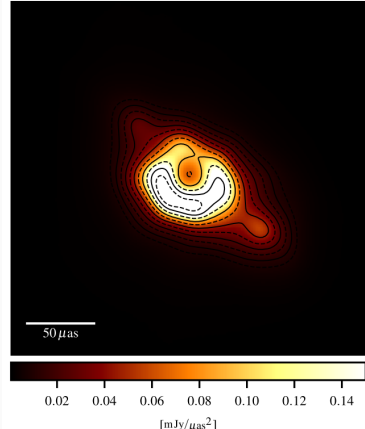


Figure 4: M87* on day 0 imaged with our algorithm [AFH⁺20]. Saturated color bar.

INFERENCE MODEL

Product Rule of Probabilities aka **Bayes' theorem**

$$\mathcal{P}(s|d, \mathcal{M}) = \frac{\mathcal{P}(d|s, \mathcal{M}) \mathcal{P}(s|\mathcal{M})}{\mathcal{P}(d|\mathcal{M})}$$

Definitions: s := parameters, d := data, \mathcal{M} : model assumptions.

Product Rule of Probabilities aka **Bayes' theorem**

$$\mathcal{P}(s|d, \mathcal{M}) = \frac{\mathcal{P}(d|s, \mathcal{M}) \mathcal{P}(s|\mathcal{M})}{\mathcal{P}(d|\mathcal{M})}$$

Definitions: s := parameters, d := data, \mathcal{M} : model assumptions.

Generative prior model: $s(\xi) = F_{\mathcal{M}}(\xi)$ with $P(\xi) = \mathcal{N}(\xi|0, 1)$

Product Rule of Probabilities aka **Bayes' theorem**

$$\mathcal{P}(\xi|d, \mathcal{M}) = \frac{\mathcal{P}(d|s(\xi), \mathcal{M}) \mathcal{N}(\xi|0, 1)}{\mathcal{P}(d|\mathcal{M})}$$

Definitions: ξ := parameters, d := data, \mathcal{M} : model assumptions.

Generative prior model: $s(\xi) = F_{\mathcal{M}}(\xi)$ with $P(\xi) = \mathcal{N}(\xi|0, 1)$

PRIOR

Sky brightness distribution

$s_{xt\nu}$ $x \in \Omega \subset \mathbb{R}^2$, $t \in I \subset \mathbb{R}$, $\nu \in V \subset \mathbb{R}^+$

Sky brightness distribution

$$S_{xt\nu} \quad x \in \Omega \subset \mathbb{R}^2, t \in I \subset \mathbb{R}, \nu \in V \subset \mathbb{R}^+$$

Prior assumptions:

Positivity, exponential scaling

$$S_{xt\nu} = e^{\tau_{xt\nu}}$$

Sky brightness distribution

$$S_{xt\nu} \quad x \in \Omega \subset \mathbb{R}^2, t \in I \subset \mathbb{R}, \nu \in V \subset \mathbb{R}^+$$

Prior assumptions:

Positivity, exponential scaling

$$S_{xt\nu} = e^{\tau_{xt\nu}}$$

Exploit correlations

$$\langle \tau_{x,t,\nu} \tau_{x',t',\nu'} \rangle_{P(\tau)} = C(x, t, \nu, x', t', \nu')$$

Sky brightness distribution

$$S_{xt\nu} \quad x \in \Omega \subset \mathbb{R}^2, t \in I \subset \mathbb{R}, \nu \in V \subset \mathbb{R}^+$$

Prior assumptions:

Positivity, exponential scaling

$$S_{xt\nu} = e^{T_{xt\nu}}$$

Exploit correlations

$$\langle \tau_{x,t,\nu} \tau_{x',t',\nu'} \rangle_{P(\tau)} = C(x, t, \nu, x', t', \nu')$$

- Independent correlations

$$= C^\Omega(x, x') C^I(t, t') C^V(\nu, \nu')$$

Sky brightness distribution

$$S_{xt\nu} \quad x \in \Omega \subset \mathbb{R}^2, t \in I \subset \mathbb{R}, \nu \in V \subset \mathbb{R}^+$$

Prior assumptions:

Positivity, exponential scaling

$$S_{xt\nu} = e^{T_{xt\nu}}$$

Exploit correlations

$$\begin{aligned} \langle \tau_{x,t,\nu} \tau_{x',t',\nu'} \rangle_{P(\tau)} &= C(x, t, \nu, x', t', \nu') \\ &= C^\Omega(x, x') C^I(t, t') C^V(\nu, \nu') \\ &= C^\Omega(|x - x'|) C^I(|t - t'|) C^V(|\nu - \nu'|) \end{aligned}$$

- Independent correlations
- Homogeneity and isotropy

Sky brightness distribution

$$S_{xt\nu} \quad x \in \Omega \subset \mathbb{R}^2, t \in I \subset \mathbb{R}, \nu \in V \subset \mathbb{R}^+$$

Prior assumptions:

Positivity, exponential scaling

$$S_{xt\nu} = e^{\tau_{xt\nu}}$$

Exploit correlations

$$\langle \tau_{x,t,\nu} \tau_{x',t',\nu'} \rangle_{P(\tau)} = C(x, t, \nu, x', t', \nu')$$

- Independent correlations

$$= C^\Omega(x, x') C^I(t, t') C^V(\nu, \nu')$$

- Homogeneity and isotropy

$$= C^\Omega(|x - x'|) C^I(|t - t'|) C^V(|\nu - \nu'|)$$

$\Rightarrow C^i$ fully determined by associated power spectrum $P^i(|k|)$ $\forall i \in \{\Omega, I, V\}$

Sky brightness distribution

$$S_{xt\nu} \quad x \in \Omega \subset \mathbb{R}^2, t \in I \subset \mathbb{R}, \nu \in V \subset \mathbb{R}^+$$

Prior assumptions:

Positivity, exponential scaling

$$S_{xt\nu} = e^{\tau_{xt\nu}}$$

Exploit correlations

$$\langle \tau_{x,t,\nu} \tau_{x',t',\nu'} \rangle_{P(\tau)} = C(x, t, \nu, x', t', \nu')$$

- Independent correlations

$$= C^\Omega(x, x') C^I(t, t') C^V(\nu, \nu')$$

- Homogeneity and isotropy

$$= C^\Omega(|x - x'|) C^I(|t - t'|) C^V(|\nu - \nu'|)$$

$\Rightarrow C^i$ fully determined by associated power spectrum $P^i(|k|)$ $\forall i \in \{\Omega, I, V\}$

Uninformative

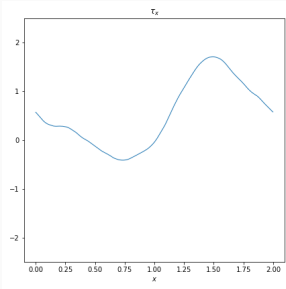
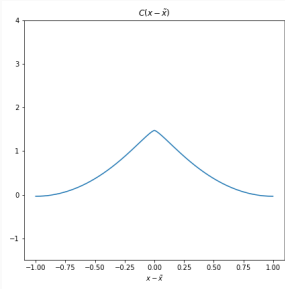
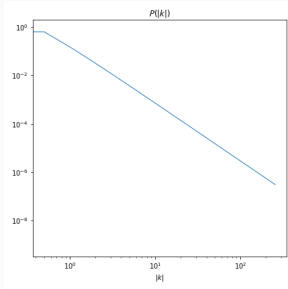
$$\Rightarrow P(\tau) = \mathcal{N}(\tau | 0, C)$$

PRIOR - CORRELATIONS

$$P^{(i)}(|k|) \quad i \in \{\Omega, I, V\}$$

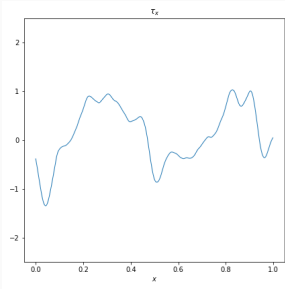
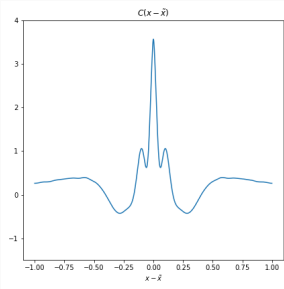
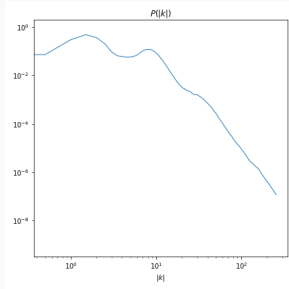
PRIOR - CORRELATIONS

$$P^{(i)}(|k|) \propto |k|^{-\alpha} \quad i \in \{\Omega, l, V\}$$



PRIOR - CORRELATIONS

$$P^{(i)}(|k|)$$



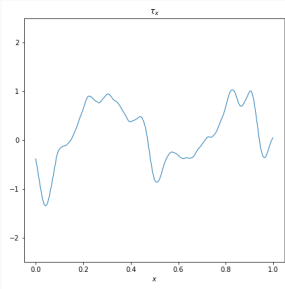
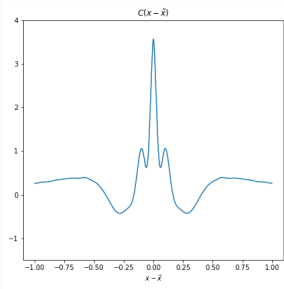
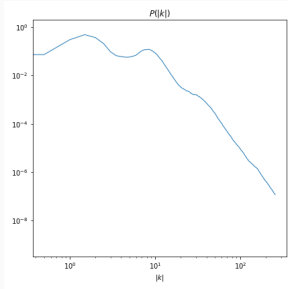
PRIOR - CORRELATIONS

$$P^{(i)}(|k|) = e^{q(l)}$$

with $l = \log(|k|)$

$$\frac{\partial^2 q}{\partial l^2} = \sigma \xi_q$$

$P(\xi_q) = \mathcal{N}(\xi_q | 0, \mathbf{1})$ Integrated Wiener Process



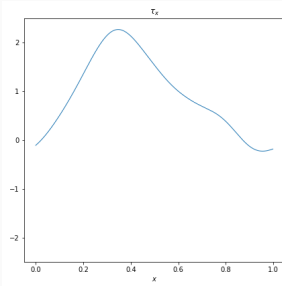
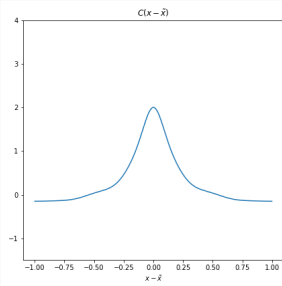
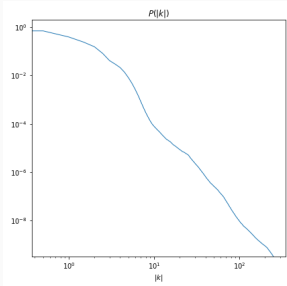
PRIOR - CORRELATIONS

$$P^{(i)}(|k|) = e^{q(l)}$$

with $l = \log(|k|)$

$$\frac{\partial^2 q}{\partial l^2} = \sigma \xi_q$$

$P(\xi_q) = \mathcal{N}(\xi_q | 0, \mathbf{1})$ Integrated Wiener Process



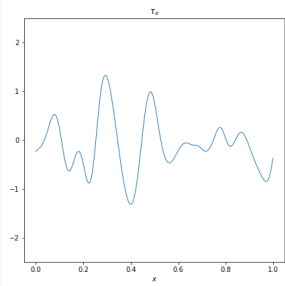
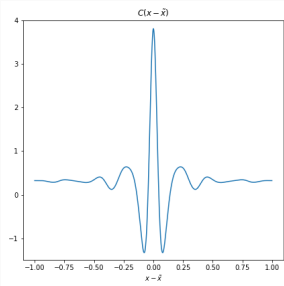
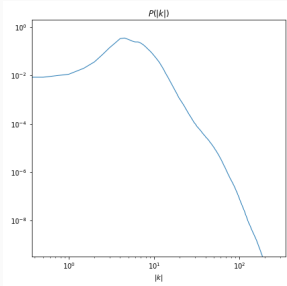
PRIOR - CORRELATIONS

$$P^{(i)}(|k|) = e^{q(l)}$$

with $l = \log(|k|)$

$$\frac{\partial^2 q}{\partial l^2} = \sigma \xi_q$$

$P(\xi_q) = \mathcal{N}(\xi_q | 0, \mathbf{1})$ Integrated Wiener Process



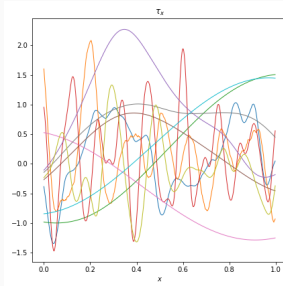
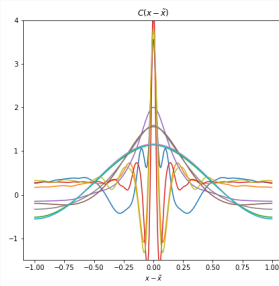
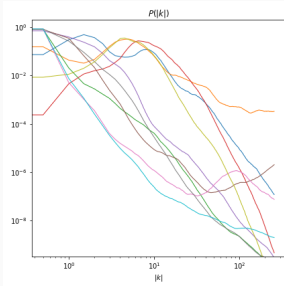
PRIOR - CORRELATIONS

$$P^{(i)}(|k|) = e^{q(l)}$$

with $l = \log(|k|)$

$$\frac{\partial^2 q}{\partial l^2} = \sigma \xi_q$$

$P(\xi_q) = \mathcal{N}(\xi_q | 0, \mathbf{1})$ Integrated Wiener Process



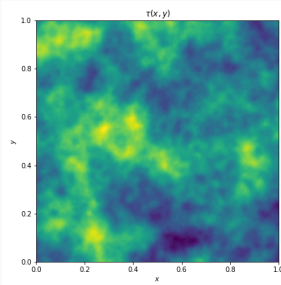
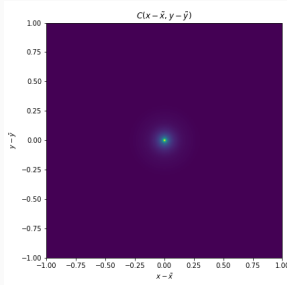
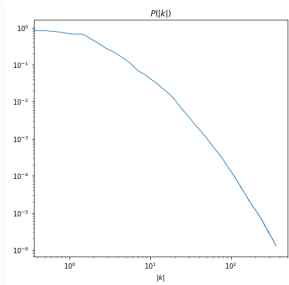
PRIOR - CORRELATIONS

$$P^{(i)}(|k|) = e^{q(l)}$$

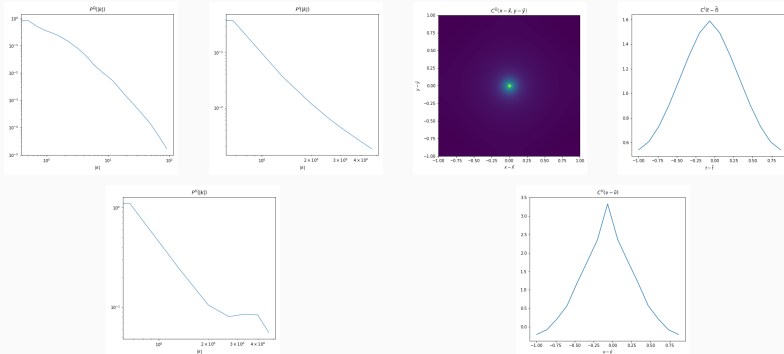
with $l = \log(|k|)$

$$\frac{\partial^2 q}{\partial l^2} = \sigma \xi_q$$

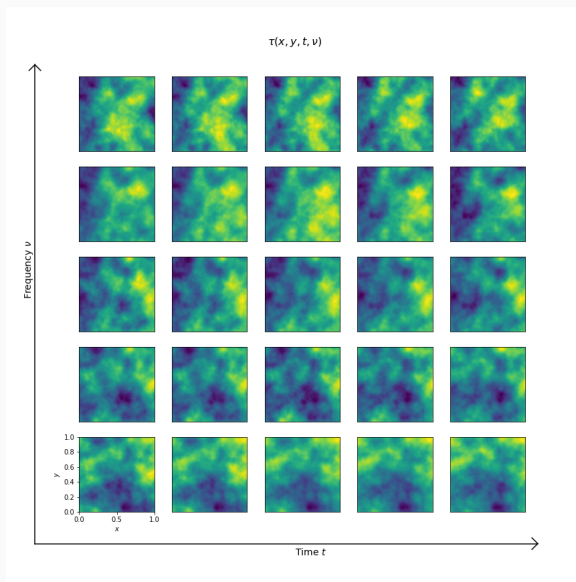
$P(\xi_q) = \mathcal{N}(\xi_q | 0, \mathbf{1})$ Integrated Wiener Process



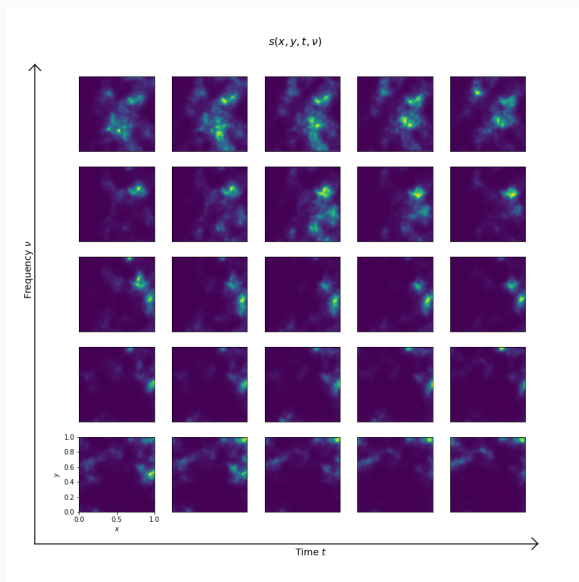
PRIOR - CORRELATIONS



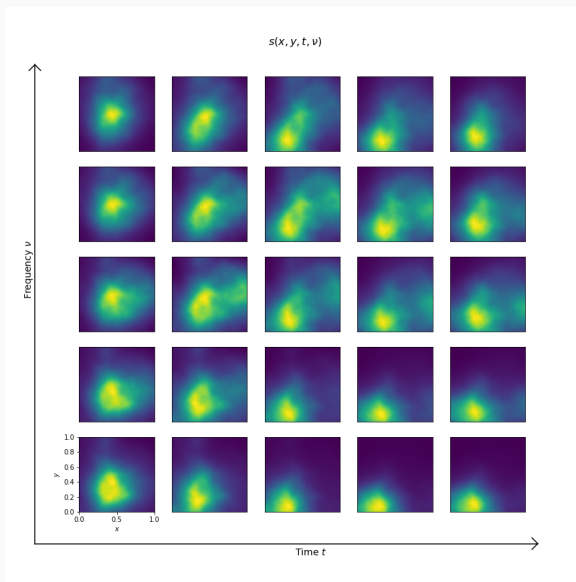
PRIOR



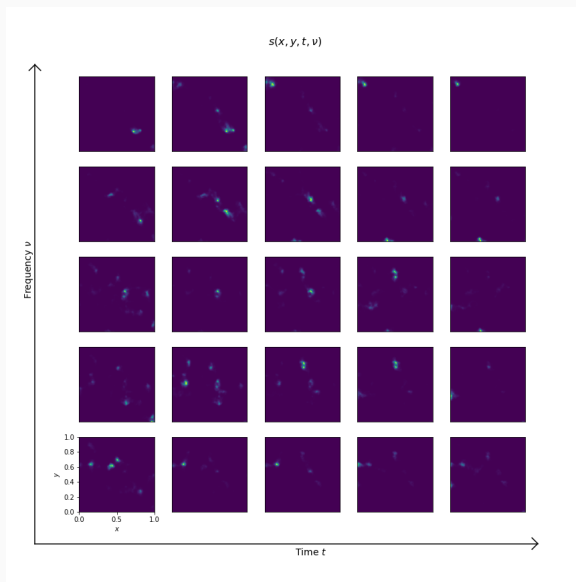
PRIOR



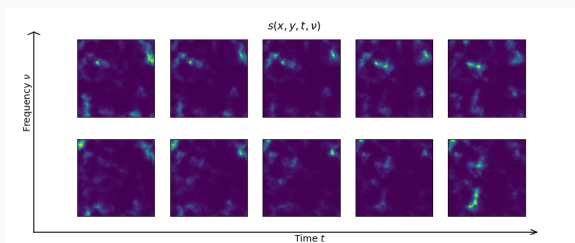
PRIOR



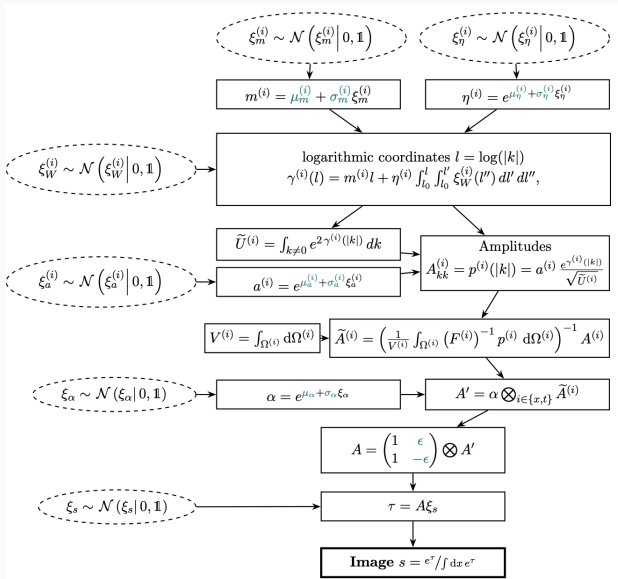
PRIOR



PRIOR

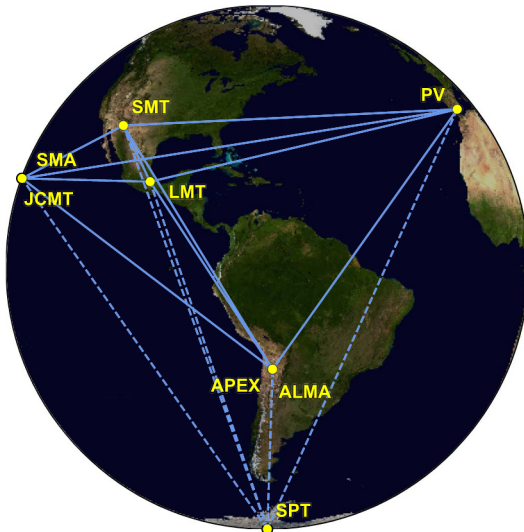


PRIOR



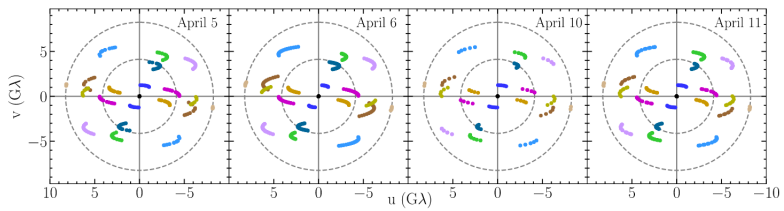
LIKELIHOOD

THE EVENT HORIZON TELESCOPE (EHT)



[AAA⁺19a]

THE EVENT HORIZON TELESCOPE (EHT)



[AAA⁺19b]

LIKELIHOOD

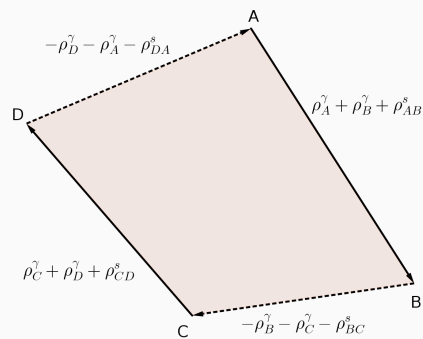
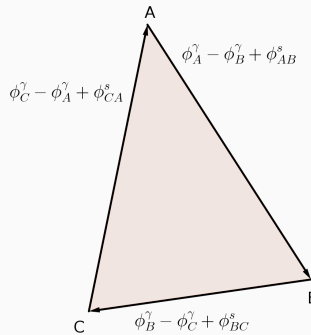
- Visibility data d and thermal noise level σ reported by [AAA⁺19a]

LIKELIHOOD

- Visibility data d and thermal noise level σ reported by [AAA⁺19a]
- Direct imaging using visibilities is challenging for VLBI

LIKELIHOOD

- Visibility data d and thermal noise level σ reported by [AAA⁺19a]
- Direct imaging using visibilities is challenging for VLBI
 \Rightarrow Imaging using closure quantities (phases ϕ^d and logarithmic amplitudes ρ^d)



$$\phi_{clos}^d = \textcolor{orange}{M} \phi^d$$

$$\rho_{clos}^d = \textcolor{orange}{L} \rho^d$$

LIKELIHOOD

$$\begin{aligned}\mathcal{P}(\phi_{clos}^d | s) &\approx \mathcal{N}(e^{i\phi_{clos}^d} | e^{i\phi_{clos}^s}, MNM^\dagger) \quad \text{with} \quad N = \text{diag}\left(\frac{\sigma^2}{|d|^2}\right) \\ \mathcal{P}(\rho_{clos}^d | s) &\approx \mathcal{N}(\rho_{clos}^d | \rho_{clos}^s, LNL^\dagger)\end{aligned}$$

$$\begin{aligned}\mathcal{P}(\phi_{\text{clos}}^d | s) &\approx \mathcal{N}\left(e^{i\phi_{\text{clos}}^d} | e^{i\phi_{\text{clos}}^s}, MNM^\dagger\right) \quad \text{with} \quad N = \text{diag}\left(\frac{\sigma^2}{|d|^2}\right) \\ \mathcal{P}(\rho_{\text{clos}}^d | s) &\approx \mathcal{N}\left(\rho_{\text{clos}}^d | \rho_{\text{clos}}^s, LNL^\dagger\right)\end{aligned}$$

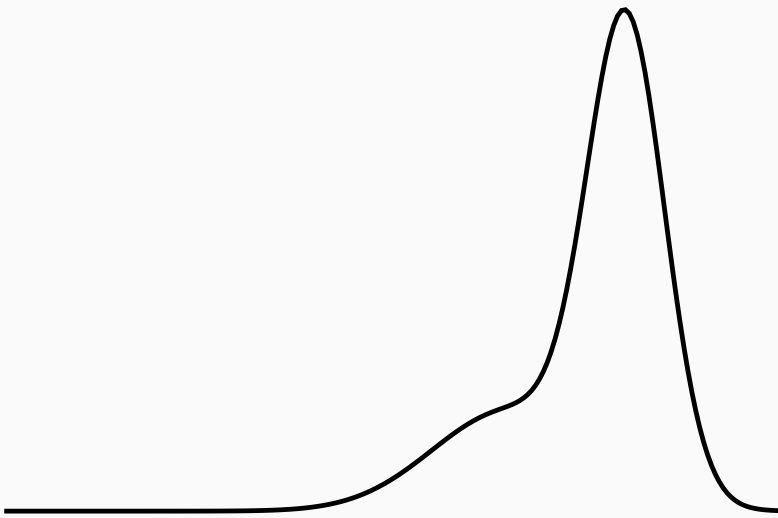
Posterior distribution

$$\mathcal{P}(\xi | \phi_{\text{clos}}^d, \rho_{\text{clos}}^d) \propto \mathcal{P}(\phi_{\text{clos}}^d | s(\xi)) \mathcal{P}(\rho_{\text{clos}}^d | s(\xi)) \mathcal{N}(\xi | 0, 1)$$

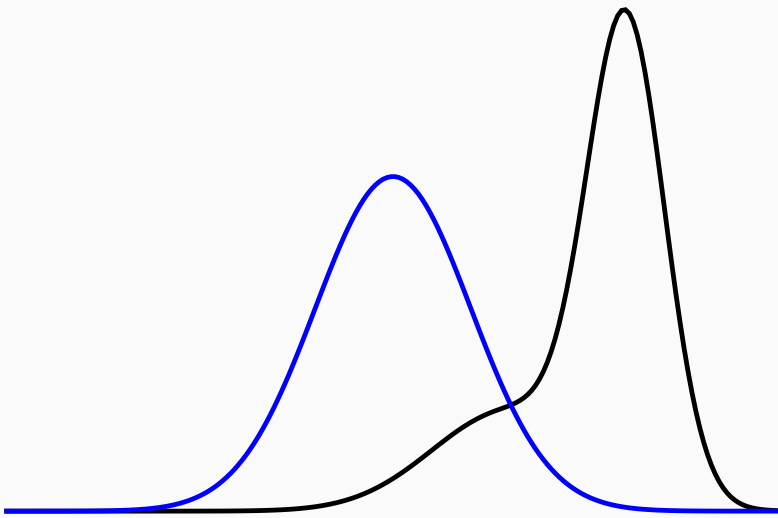
with generative prior $s(\xi) = F_M(\xi)$

METRIC GAUSSIAN VARIATIONAL INFERENCE

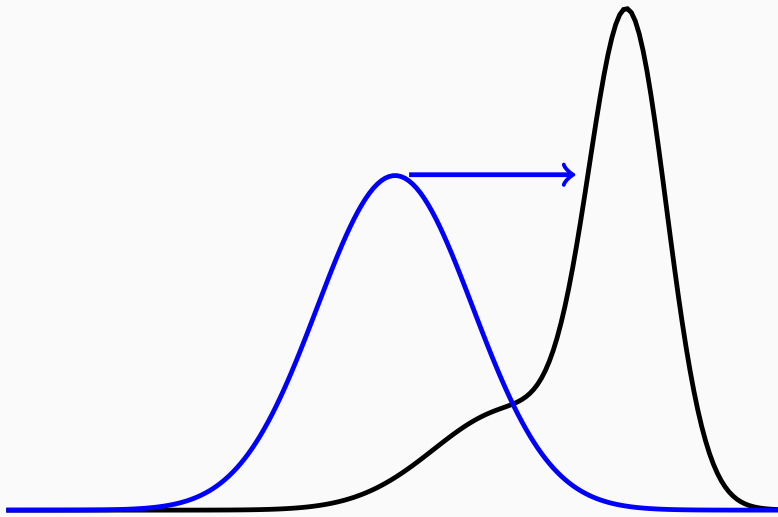
VARIATIONAL INFERENCE



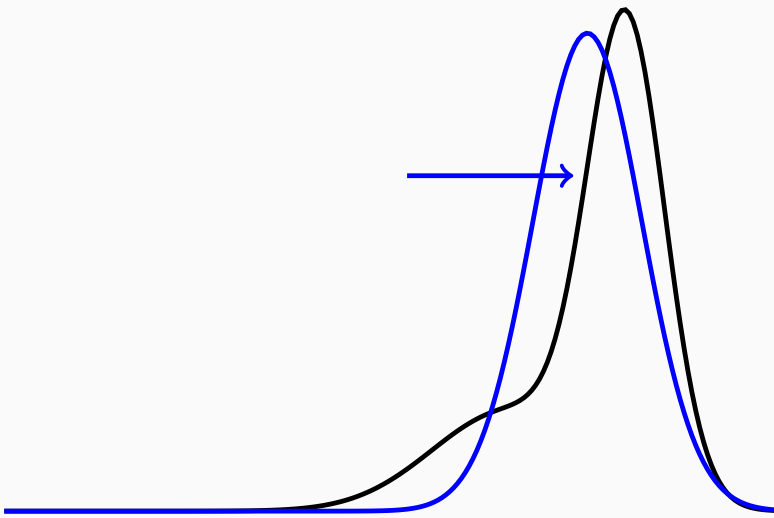
VARIATIONAL INFERENCE



VARIATIONAL INFERENCE



VARIATIONAL INFERENCE



Kullback-Leibler Divergence

$$\mathcal{D}_{\text{KL}}(\mathcal{Q}_\eta(\xi) \parallel \mathcal{P}(\xi|d)) = \int d\xi \mathcal{Q}_\eta(\xi) \ln \frac{\mathcal{Q}_\eta(\xi)}{\mathcal{P}(\xi|d)}$$

$$Q_\eta(\xi) = \mathcal{N}(\xi | \bar{\xi}, \Xi)$$

$$Q_\eta(\xi) = \mathcal{N}(\xi | \bar{\xi}, \Xi)$$

$$\Xi = \begin{pmatrix} \cdot & \cdot & \cdot & \cdot \\ \cdot & \cdot & \cdot & \cdot \\ \cdot & \cdot & \cdot & \cdot \\ \cdot & \cdot & \cdot & \cdot \end{pmatrix}$$

full-covariance

$$Q_\eta(\xi) = \mathcal{N}(\xi | \bar{\xi}, \Xi)$$

$$\Xi = \begin{pmatrix} \ddots & & & \\ & \ddots & & \\ & & \ddots & \\ & & & \ddots \end{pmatrix}$$

mean-field

$$Q_\eta(\xi) = \mathcal{N}(\xi | \bar{\xi}, \Xi)$$

$$\Xi(\xi) = (J(\xi)^\dagger I_d(\theta) J(\xi) + \mathbb{1})^{-1}$$

inverse Fisher metric

$$Q_\eta(\xi) = \mathcal{N}(\xi | \bar{\xi}, \Xi)$$

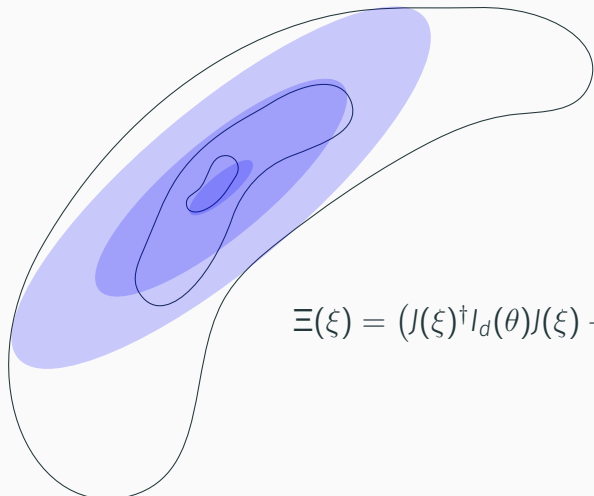
$$\Xi(\xi) = (J(\xi)^\dagger I_d(\theta) J(\xi) + \mathbb{1})^{-1}$$

inverse Fisher metric

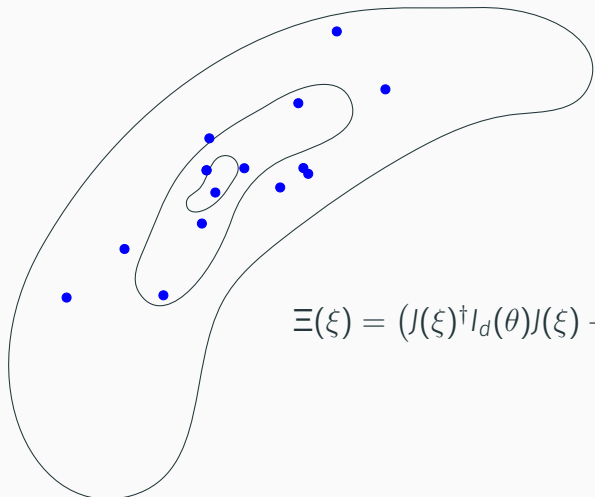
$$J(\xi) = \frac{\partial \theta(\xi)}{\partial \xi}$$

$$I_d(\theta) = \left\langle \frac{\partial \mathcal{H}(d|\theta)}{\partial \theta} \frac{\partial \mathcal{H}(d|\theta)}{\partial \theta^\dagger} \right\rangle_{\mathcal{P}(d|\theta)}$$

METRIC GAUSSIAN VARIATIONAL INFERENCE

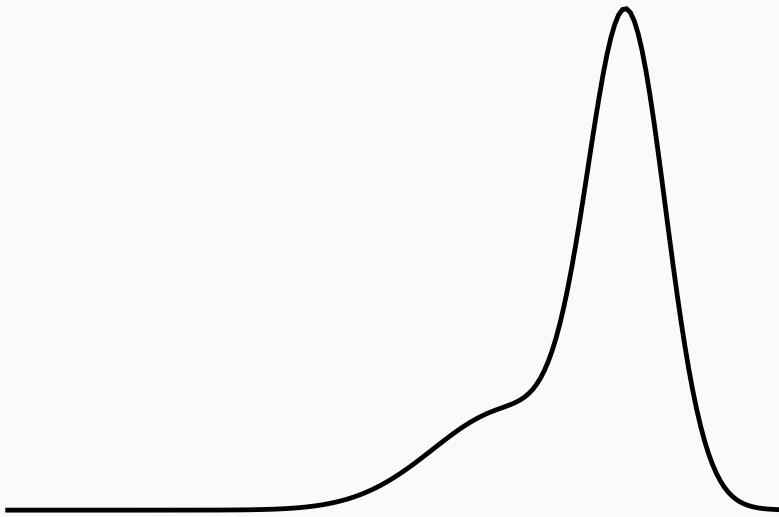


METRIC GAUSSIAN VARIATIONAL INFERENCE

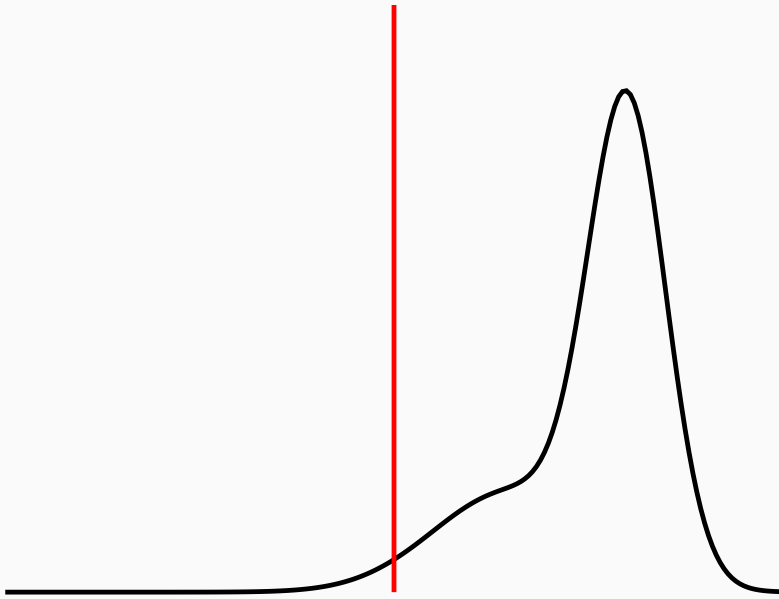


$$\Xi(\xi) = \left(J(\xi)^\dagger I_d(\theta) J(\xi) + \mathbb{1} \right)^{-1}$$

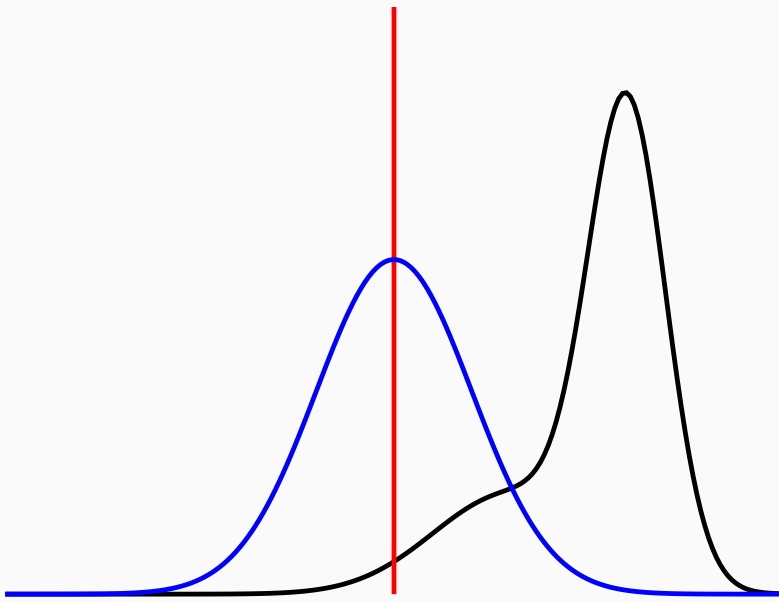
METRIC GAUSSIAN VARIATIONAL INFERENCE



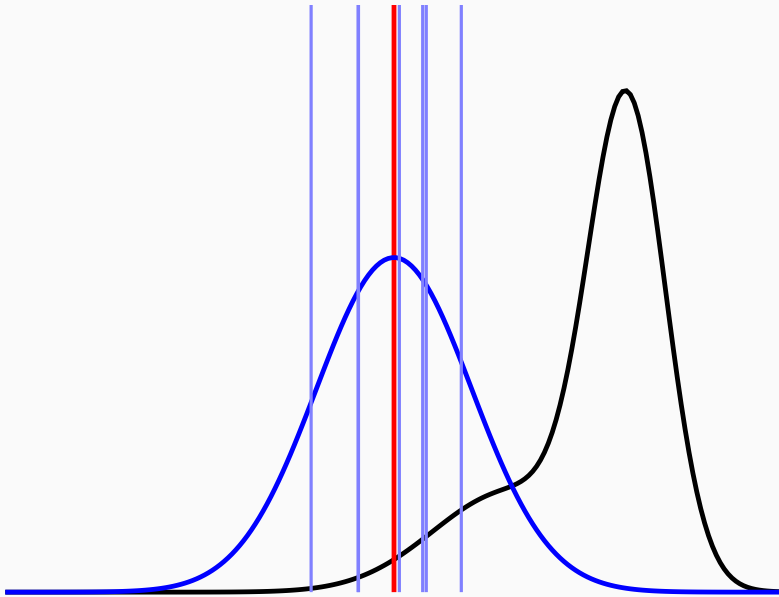
METRIC GAUSSIAN VARIATIONAL INFERENCE



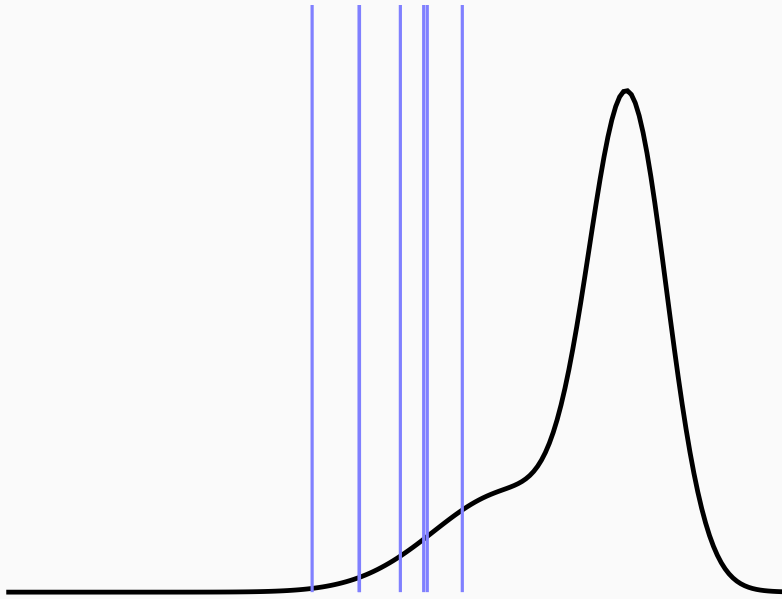
METRIC GAUSSIAN VARIATIONAL INFERENCE



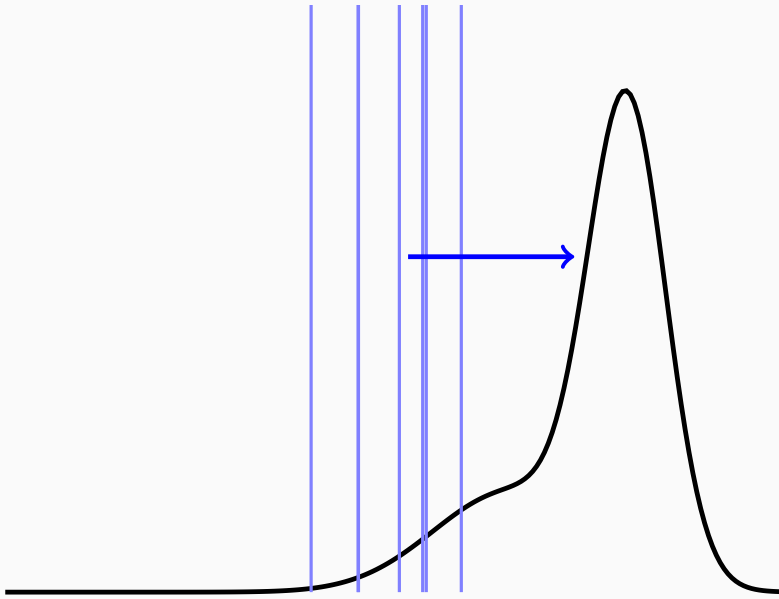
METRIC GAUSSIAN VARIATIONAL INFERENCE



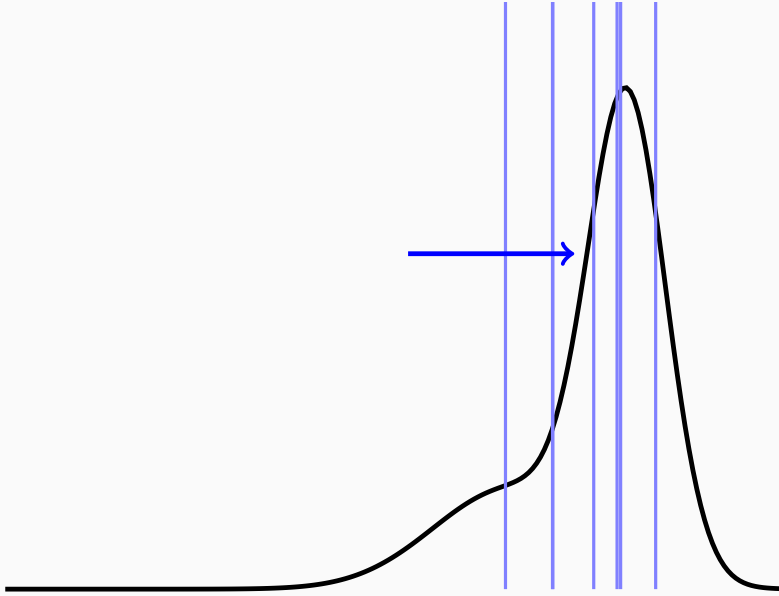
METRIC GAUSSIAN VARIATIONAL INFERENCE



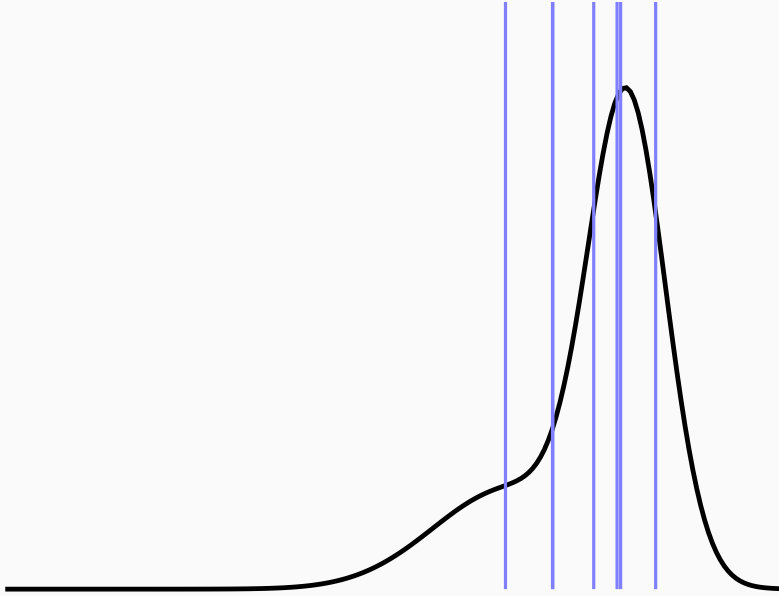
METRIC GAUSSIAN VARIATIONAL INFERENCE



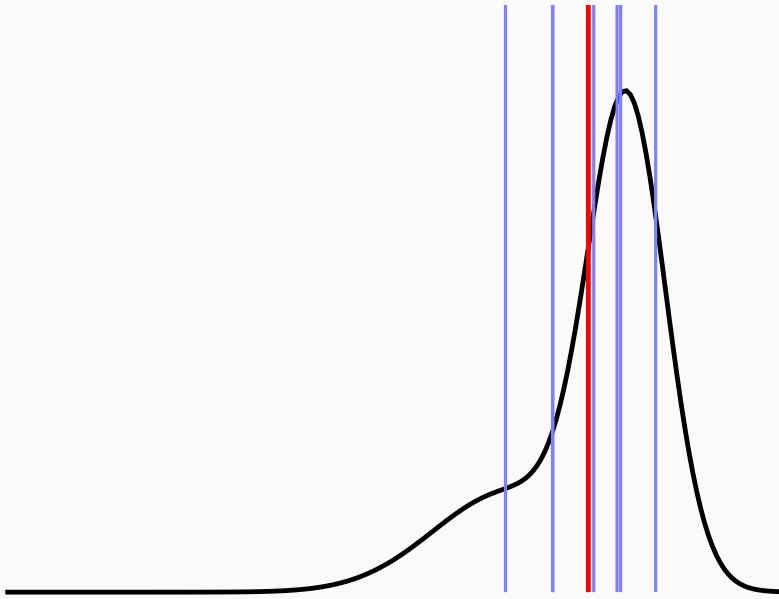
METRIC GAUSSIAN VARIATIONAL INFERENCE



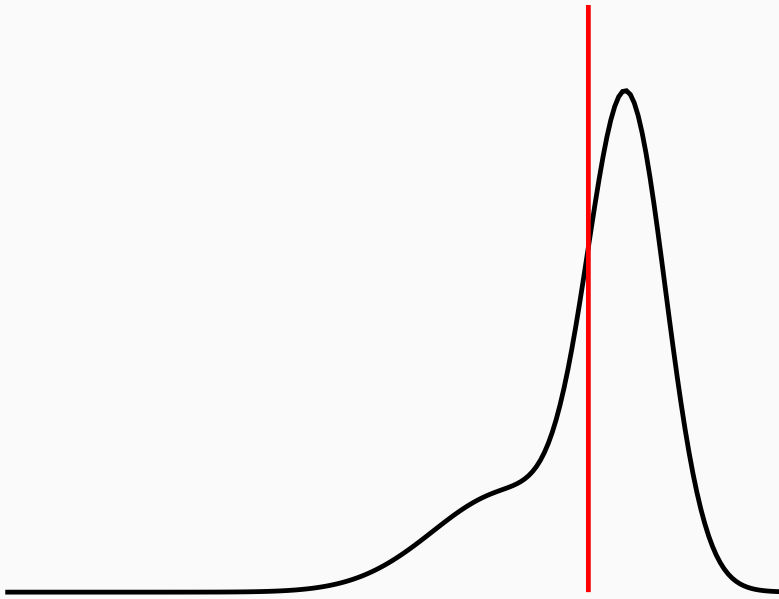
METRIC GAUSSIAN VARIATIONAL INFERENCE



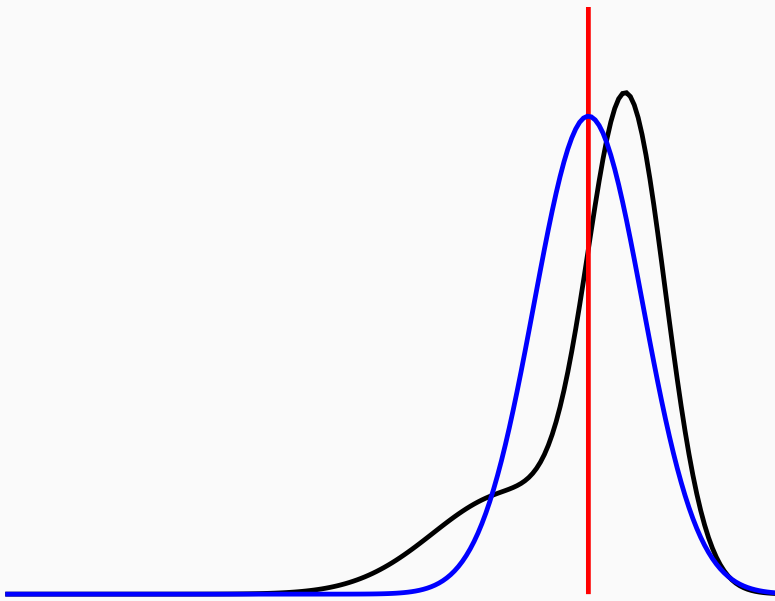
METRIC GAUSSIAN VARIATIONAL INFERENCE



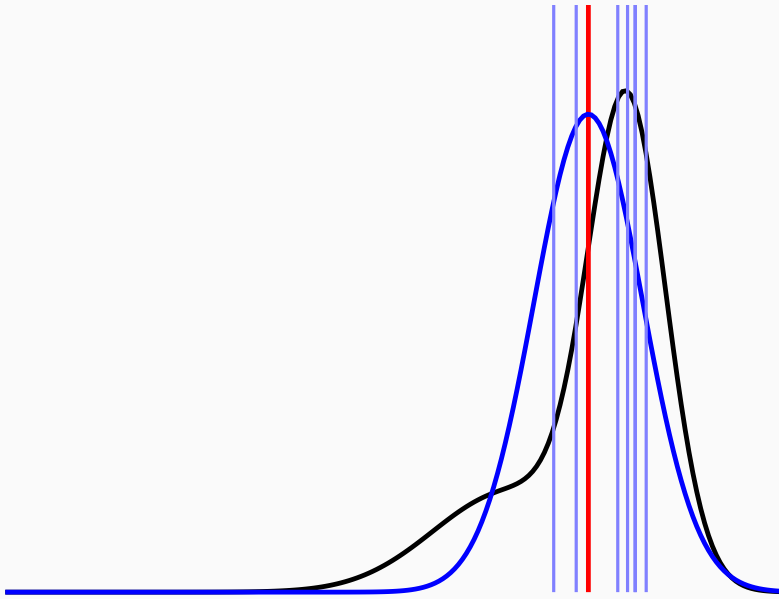
METRIC GAUSSIAN VARIATIONAL INFERENCE



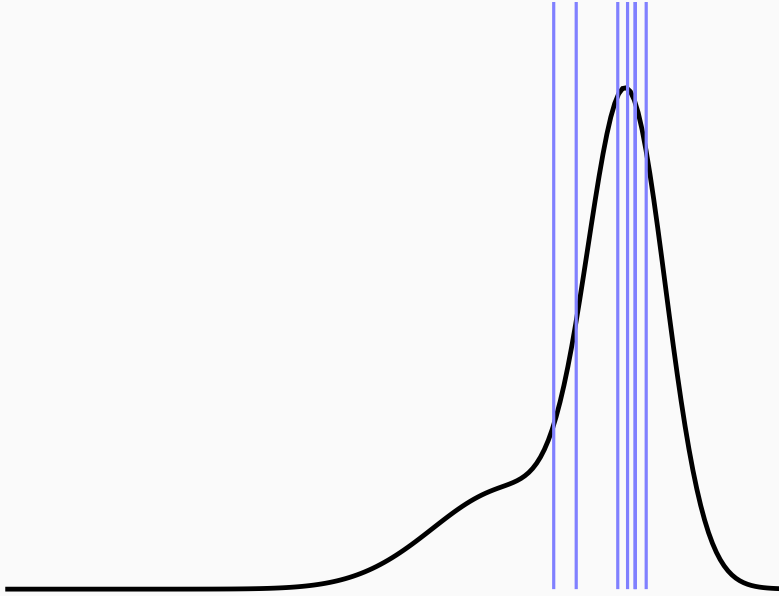
METRIC GAUSSIAN VARIATIONAL INFERENCE



METRIC GAUSSIAN VARIATIONAL INFERENCE

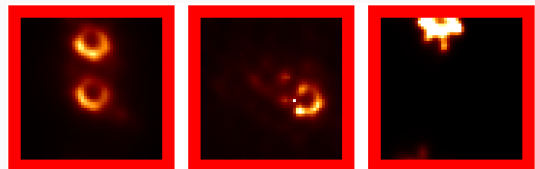


METRIC GAUSSIAN VARIATIONAL INFERENCE



PRACTICAL CHALLENGES FOR VLBI

- Nonlinear optimization
- Stochastic loss function
- No absolute source position or brightness
- Multi-modality
 - Multiple source copies
 - “Source Teleportation”



INFERENCE HEURISTIC

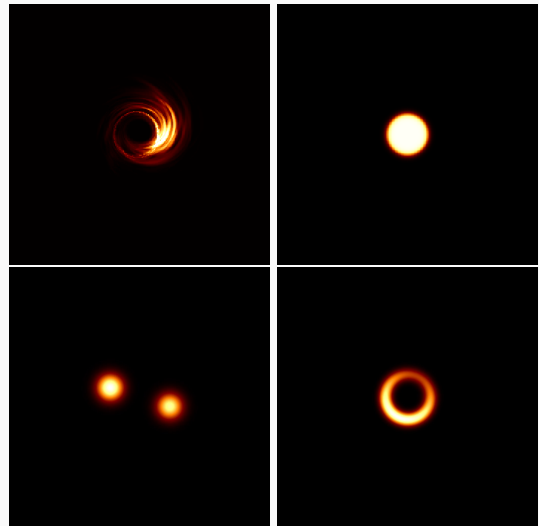
- Initially fit model to Gaussian shape
- Start with data of the first two days
- Alternate between phase and amplitude likelihood
- Reduce stochasticity of loss towards the end

Iteration	Data Set	Tempering	Optimizer	Sample Pairs
$i = 0$	$i \ge 0$	$i \ge 0$	$i \ge 0$	$i \ge 0$
	first two days	full likelihood	V-LBFGS $4 * (4 + i/4)$ iterations	
		$i \ge 10$		
	$i \ge 30$	alternating		
				$N = 10 * (1 + i/8)$
	all days	$i \ge 50$	$i \ge 50$	
		full likelihood	Natural Gradient 20 iterations	
$i = 59$				

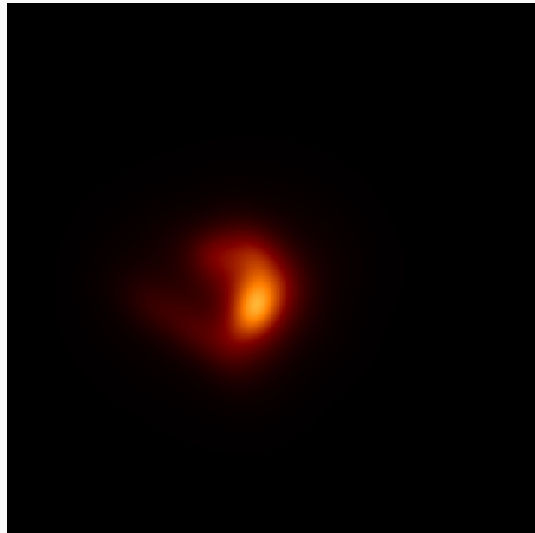
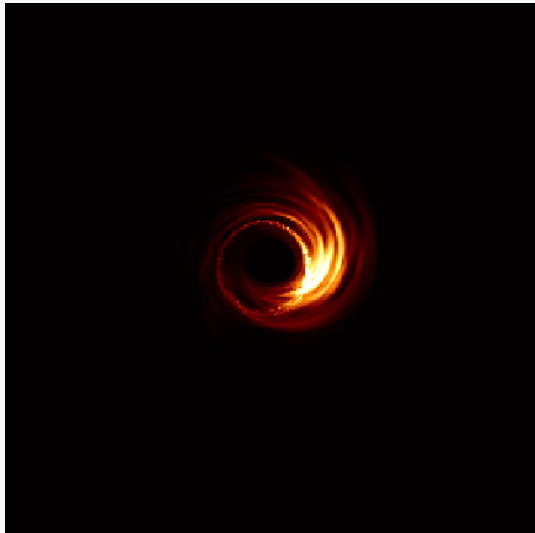
VALIDATION

STRATEGY

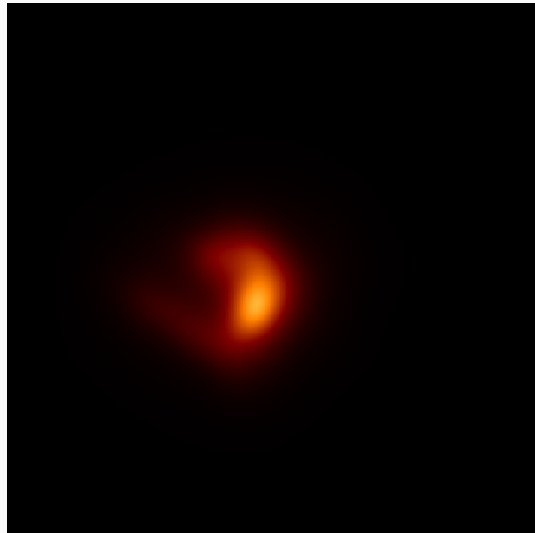
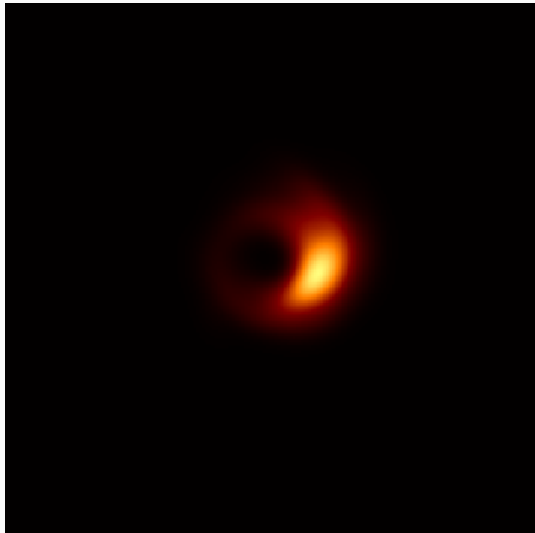
- Synthetic source
- Generate data according to EHT observation
- Reconstruct
- Compare to truth



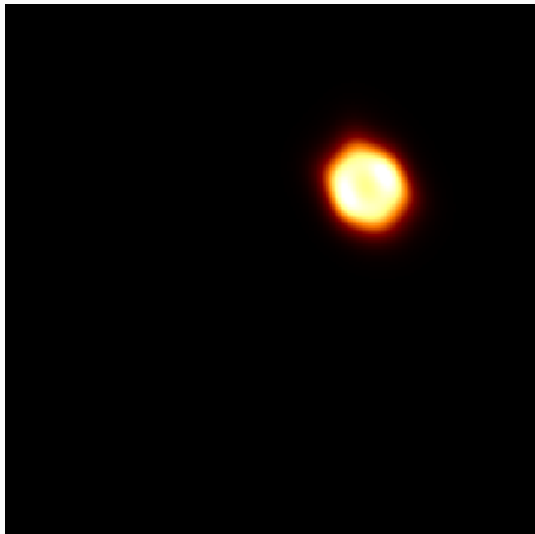
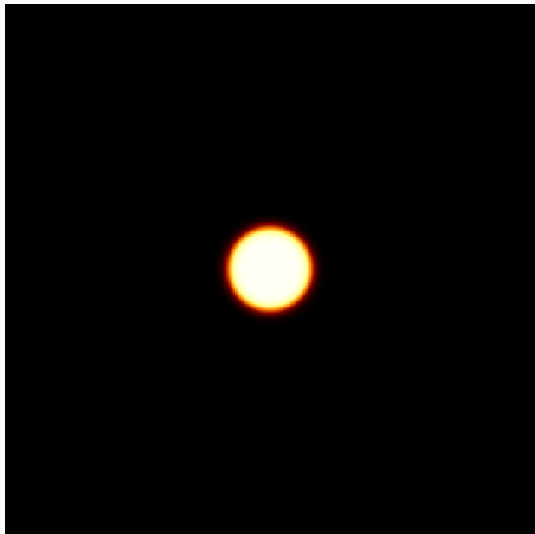
STATIC SOURCE: SIMULATION



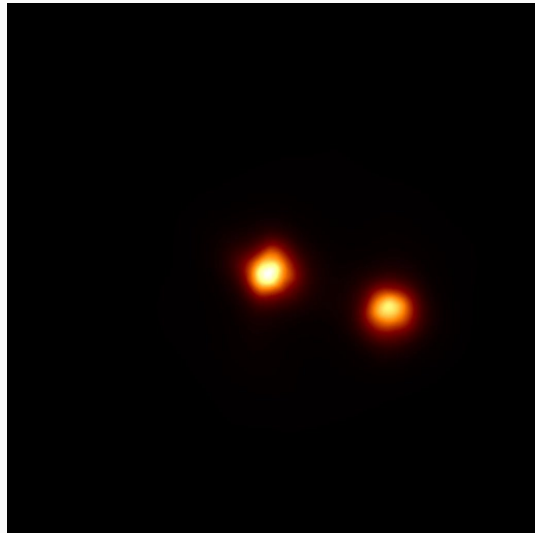
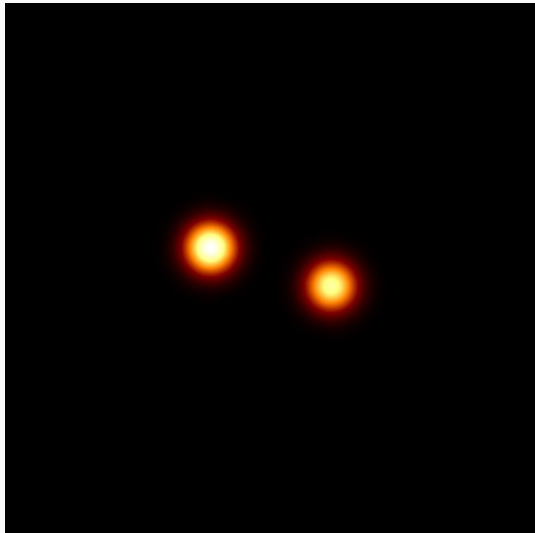
STATIC SOURCE: SIMULATION



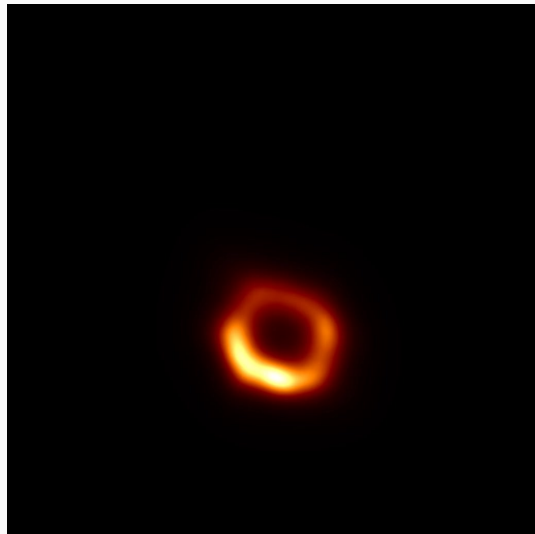
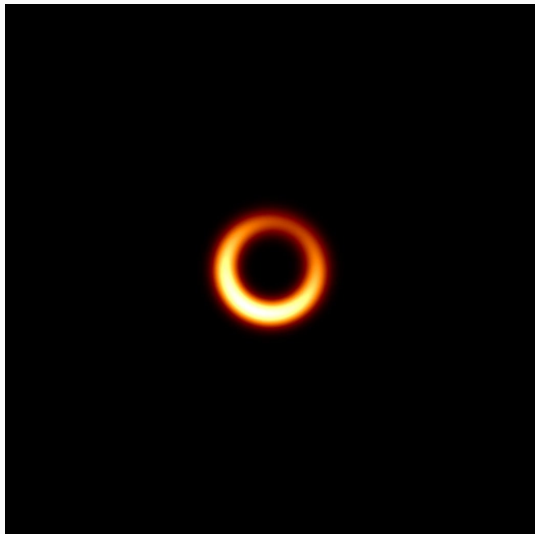
STATIC SOURCE: DISK



DYNAMIC SOURCE: GAUSSIAN SHAPES

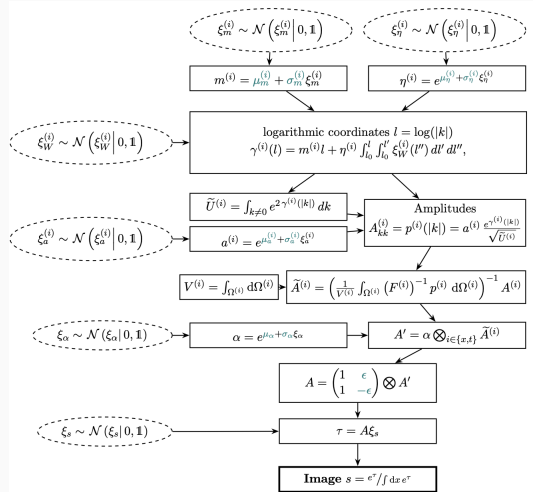


DYNAMIC SOURCE: CRESCENT



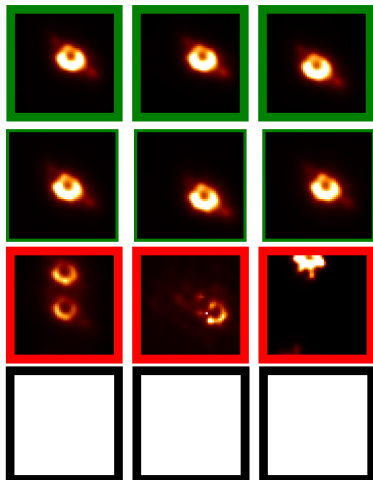
HYPERPARAMETER VALIDATION

- In total 15 hyperparameters
- Specifying mean and variance
- Draw mean hyperparameters within a uniform 3σ interval
- Perform 100 reconstructions

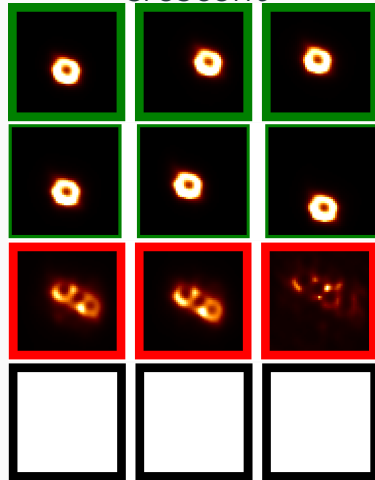


THE GOOD, THE BAD AND THE UGLY

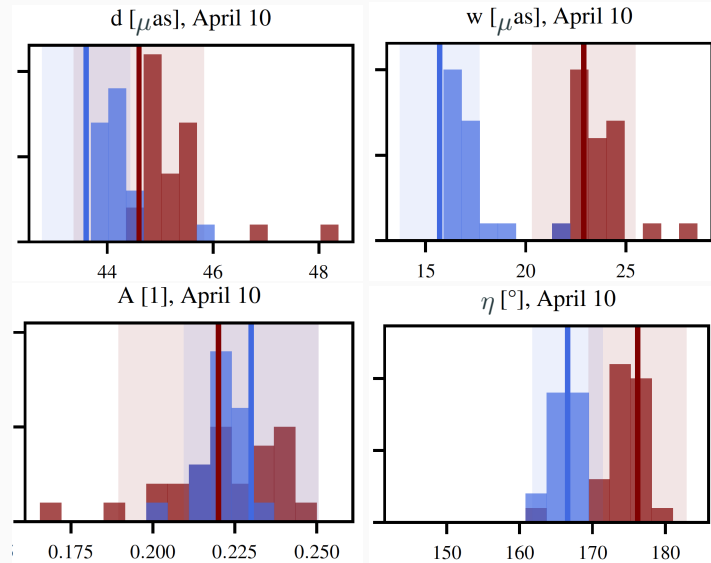
M87*



Crescent

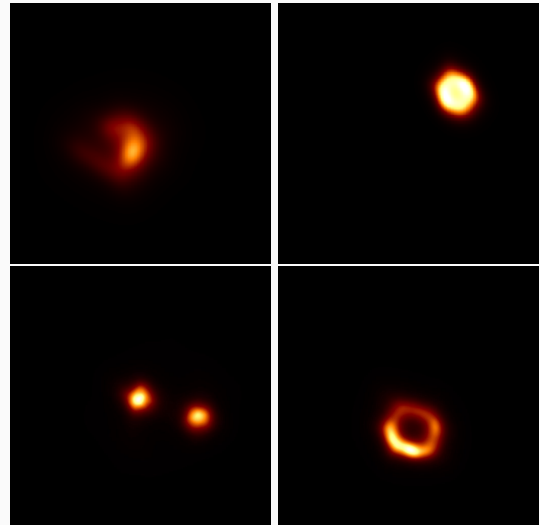


RING PARAMETERS



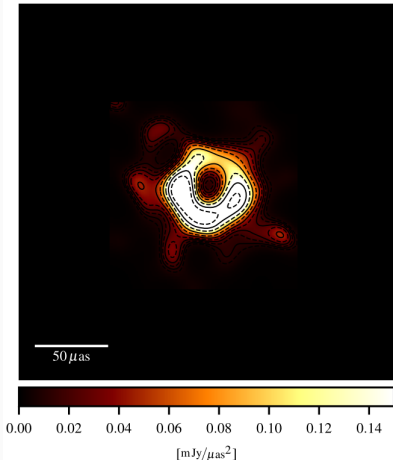
VALIDATION

- Reconstruction works on various sources
- We recover dynamics
- Results are widely insensitive to hyperparameters
- Room for improvement in the inference heuristic



CONCLUSION

CONCLUSION

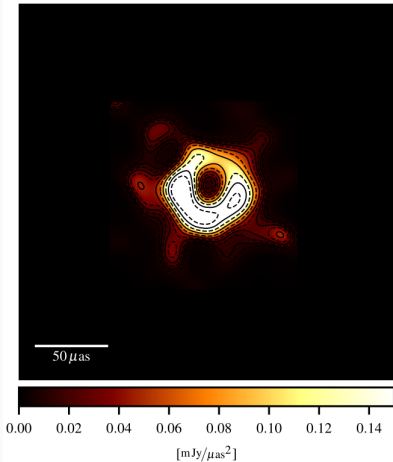


Differences to [AAA⁺19b]

- Uncertainty quantification via multiple independent imaging teams
- Independent imaging for each observing day

Figure 5: M87* on day 0 imaged with ehtimaging [AAA⁺19b]. Saturated color bar.

CONCLUSION

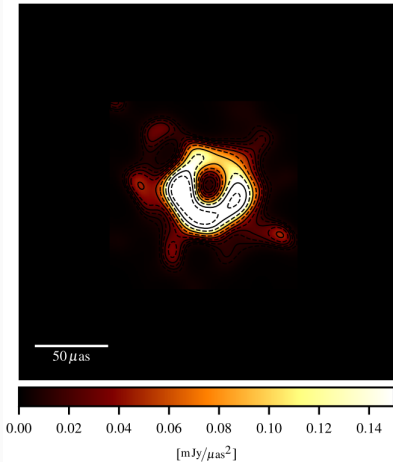


Differences to [AAA⁺19b]

- Intrinsic uncertainty quantification
- Independent imaging for each observing day

Figure 5: M87* on day 0 imaged with ehtimaging [AAA⁺19b]. Saturated color bar.

CONCLUSION

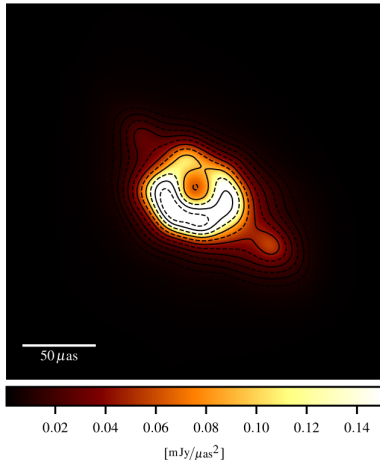


Differences to [AAA⁺19b]

- Intrinsic uncertainty quantification
- Temporal correlations → full 4d-movie

Figure 5: M87* on day 0 imaged with ehtimaging [AAA⁺19b]. Saturated color bar.

CONCLUSION



Differences to [AAA⁺19b]

- Intrinsic uncertainty quantification
- Temporal correlations → full 4d-movie

Figure 5: M87* on day 0 imaged with *vlbi-resolve* [AFH⁺20]. Saturated color bar.

CONCLUSION

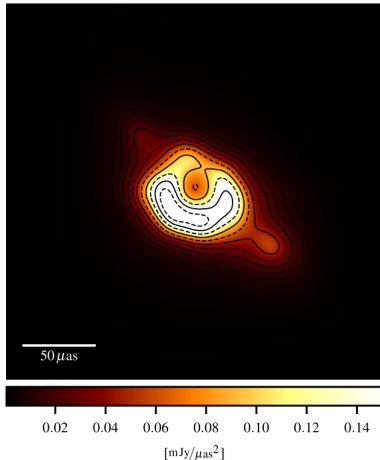


Figure 5: M87* on day 0 imaged with **vlbi-resolve** [AFH⁺20]. Saturated color bar.

Differences to [AAA⁺19b]

- Intrinsic uncertainty quantification
- Temporal correlations → full 4d-movie

Some aspects

- **Four-dimensional** (time, frequency, space) reconstruction of M87*
- **Correlation kernel** is non-parametrically learned from the data
- **Bayesian** treatment despite huge problem size (10^7 dofs)

QUESTIONS? DISCUSSION!

REFERENCES

-  Kazunori Akiyama, Antxon Alberdi, Walter Alef, Keiichi Asada, Rebecca Azulay, Anne-Kathrin Baczko, David Ball, Mislav Baloković, John Barrett, Dan Bintley, et al.
First M87 Event Horizon Telescope Results. I. The Shadow of the Supermassive Black Hole.
The Astrophysical Journal Letters, 875(1):L1, April 2019.
-  Kazunori Akiyama, Antxon Alberdi, Walter Alef, Keiichi Asada, Rebecca Azulay, Anne-Kathrin Baczko, David Ball, Mislav Baloković, John Barrett, Dan Bintley, et al.
First M87 Event Horizon Telescope Results. IV. Imaging the Central Supermassive Black Hole.
The Astrophysical Journal Letters, 875(1):L4, April 2019.
-  Philipp Arras, Philipp Frank, Philipp Haim, Jakob Knollmüller, Reimar Leike, Martin Reinecke, and Torsten Enßlin.
M87* in space, time, and frequency.
arXiv e-prints, page arXiv:2002.05218, February 2020.

SPECTRAL DEPENDENCY

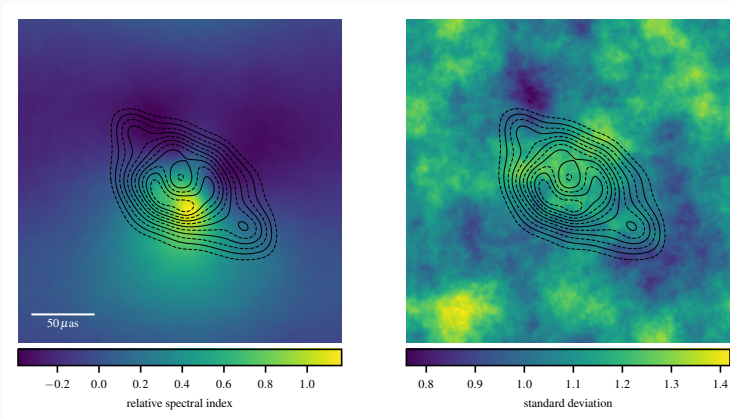


Figure 6: The relative spectral index and the pixel-wise uncertainty, as calculated from the 227–229 GHz channels.

REDUCED χ^2

	April 5	April 6	April 10	April 11
Simulation	1.2, 1.0	1.3, 1.2	1.4, 1.3	1.1, 1.1
Disk	1.6, 1.2	1.4, 1.3	1.5, 1.4	1.3, 1.2
Double Sources	1.2, 1.1	1.2, 1.1	1.3, 1.3	1.4, 1.1
Crescent	1.2, 1.0	1.3, 0.9	1.0, 0.9	1.4, 1.1
M87*	1.1, 0.9	1.1, 0.8	1.1, 0.9	1.1, 0.9

Table 1: The χ^2 of the reconstruction for closure (phase, amplitude).